Production and Detection of Randall-Sundrum Light Radions at Hadron Colliders

Uma Mahanta† and Anindya Datta♡
Mehta Research Institute, Chhatnag Road,
Jhusi, Allahabad-211019, India

e-mail: † mahanta@mri.ernet.in, ♡ anindya@mri.ernet.in

Abstract

In this paper we use the conformal anomaly in QCD to derive the coupling of light radion to gluons in the Randall-Sundrum model and use it to compute the radion production cross section at hadron colliders by gluon fusion. We find that the radion production cross section by gluon fusion at LHC would exceed that of the higgs boson by a factor that lies between 7 and 8 over most of the range. The decay modes of the radion are similar to that of the SM higgs boson. But the striking feature is the enhancement of radion to 2-photon and radion to 2-gluon branching ratio over the SM case. Utilising this, we then discuss the possible search strategies of such scalars at Tevatron and LHC. Using the $\gamma\gamma$ decay mode one can explore/exclude radion mass upto 1 TeV. Even with the current collected data at the Tevatron, one can exclude radion mass upto 120 GeV for $\langle\phi\rangle$= 1 TeV.

PACS number(s):

1 Couplings and Decay of the Radion to the SM particles

Recently Goldberger and Wise showed that the modulus in the Randall-Sundrum [1] scenario can be stabilized [2] by introducing a scalar field in the bulk. The stabilized modulus turns out to be very light if its mass arises from a small bulk scalar mass. It was shown subsequently [3] that the radion couples to the SM fields on the visible brane via the trace of the energy momentum tensor. In this article we shall study the production and decay of such a light radion at hadron colliders.

The radion couples to the SM particles on the visible brane as given in [3]

via the relation, $\mathcal{L}_{int} = \frac{1}{\langle\phi\rangle} T^\mu_\mu \tilde{\phi}$ where T^μ_μ is the trace of the symmetrized and conserved energy momentum tensor for SM fields. At the tree level it is given by,

$$T^\mu_\mu = \sum_f m_f \bar{f} f + 2M_z^2 Z^\mu Z_\mu + 2M_w^2 W^\mu W_\mu + 2m_h^2 h^2. \tag{1}$$

The fermion and gauge boson terms show the scale breaking effects due to electroweak symmetry breaking. Since the gluons and photons are massless the radion does not couple to these at the tree level. However the running of the gauge coupling in QCD and QED breaks the scale invariance and induces a trace anomaly [4]. The trace anomaly in QCD therefore generates the radion coupling to gluons which is given by

$$\mathcal{L}_{\tilde{\phi}gg} = \frac{1}{\langle\phi\rangle} \frac{\beta(g_s)}{2g_s} \tilde{\phi} G^{a\mu\nu} G^a_{\mu\nu}. \tag{2}$$

where $\frac{\beta(g_s)}{2g_s} = -(11 - \frac{2}{3}n_f)\frac{g_s^2}{32\pi^2}$. $G^a_{\mu\nu} = [\partial_\mu g^a_\nu - \partial_\nu g^a_\mu + g f^{abc} g^b_\mu g^c_\nu]$ is the gluon field strength tensor. For $m^2_{\tilde{\phi}} < 4m_t^2$ we have $n_f = 5$ dynamical quarks and hence $\frac{\beta(g_s)}{2g_s} \approx -3.84\frac{\alpha_s}{4\pi}$. On the other hand for $m^2_{\tilde{\phi}} > 4m_t^2$ we have $n_f = 6$ and hence $\frac{\beta(g_s)}{g_s} \approx -3.50\frac{\alpha_s}{4\pi}$. The anomaly contribution is independent of fermion mass. Even if EW symmetry were exact and all fermions had remained massless the trace anomaly would still lead to the above coupling of $\tilde{\phi}$ to gluons. In the presence of EWSB, heavy quark loops give rise to a contribution to $\mathcal{L}_{\tilde{\phi}gg}$. In the infinite mass limit this contribution can be obtained by replacing v by $\langle\phi\rangle$ in the effective Lagrangian for hgg coupling [eqn. 10]. It can be shown that this contribution is smaller than the anomaly contribution written above. The running of QED coupling also introduces a conformal anomaly. This gives rise to the following coupling of the radion to the photons.

$$\mathcal{L}_{\tilde{\phi}\gamma\gamma} = \frac{1}{\langle\phi\rangle} \frac{\beta(e)}{2e} \tilde{\phi} F_{\mu\nu} F^{\mu\nu} \tag{3}$$

Where $F^{\mu\nu}$ has the usual meaning. We have used the following values of $\frac{\beta(e)}{2e}$ in our calculation.

$$\begin{aligned} \frac{\beta(e)}{2e} &= \frac{13\alpha}{12\pi} \qquad m_{\tilde{\phi}} > 2m_t \\ &= \frac{31\alpha}{36\pi} \qquad 2m_t > m_{\tilde{\phi}} > 2m_W \\ &= \frac{10\alpha}{9\pi} \qquad m_{\tilde{\phi}} < 2m_W \end{aligned} \tag{4}$$

We want to mention that in the SM, in the heavy quark limit, the $h\gamma\gamma$ coupling is given by,

$$\mathcal{L}_{h\gamma\gamma} = \frac{1}{v}\frac{\beta(e)}{2e} h F_{\mu\nu}F^{\mu\nu} \tag{5}$$

where,

$$\frac{\beta(e)}{2e} = \frac{2\alpha}{9\pi} \tag{6}$$

Hence for $m^2_{\tilde{\phi}}, m^2_h < 4\, m^2_w$ (where $\tilde{\phi} \to \gamma\gamma$ is significant and the heavy top limit is valid) we have $\frac{g_{\tilde{\phi}\gamma\gamma}}{g_{h\gamma\gamma}} = 5\frac{v}{\langle\phi\rangle}$. Although $\tilde{\phi}f\bar{f}$ and $\tilde{\phi}VV$ $(V = W, Z)$ couplings are suppressed relative to $hf\bar{f}$ and hVV couplings for $\langle\phi\rangle = 1$ TeV, $\tilde{\phi}gg$ and $\tilde{\phi}\gamma\gamma$ couplings are slightly enhanced relative to hgg and $h\gamma\gamma$ couplings.

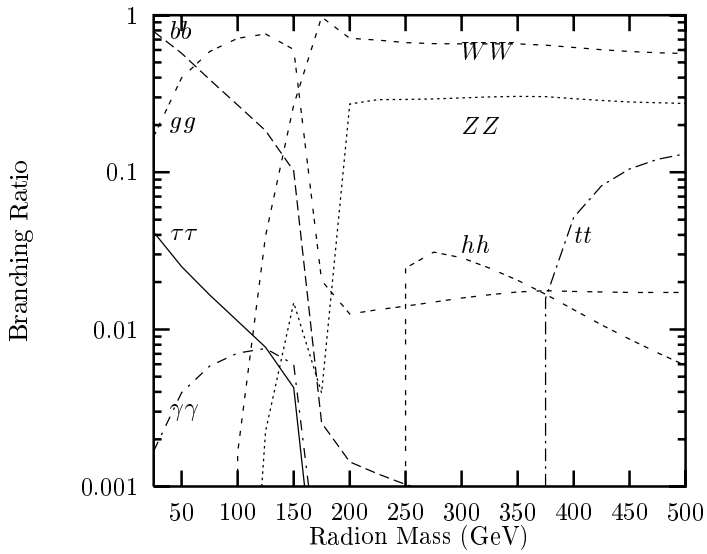

Figure 1: *Branching ratio of Radion into different channels for $\langle\phi\rangle = 1$ TeV*

Now we are in a position to present the radion decay branching ratios into different channels. In fig. 1, we present the relevant decay branching ratios. For the illustrative purpose we assumed $\langle\phi\rangle = 1$ TeV. The radion coupling to any SM field has the $\frac{1}{\langle\phi\rangle}$ dependence. Thus if we choose a different value of $\langle\phi\rangle$, the

partial decay widths of different channels change in the same fashion. But the branching ratios remain unchanged. The striking feature is that, for some radion masses the gluon gluon branching ratio is almost equal to 1. The other thing to note is that the photon photon branching ratio is also 5 to 8 times larger than the 2 photon branching ratio of the SM higgs. We see in the next section that this will have some interesting consequence in radion search. In this plot the SM higgs mass of 120 GeV is used for the purpose of illustration. This value of the SM higgs is well above the current experimental lower bound from the LEP [5]. Another interesting feature of this plot is that the radion branching ratio into gg or $\gamma\gamma$ increases slowly with $m_{\tilde{\phi}}$ after the sharp fall around WW threshold. On the contrary the higgs branching ratio in these two modes decreases with m_h after the WW threshold.

2 Radion Production at Hadron Colliders

The radion coupling to weak gauge bosons are suppressed relative to hWW and hZZ couplings by a factor of $\frac{v}{\langle\phi\rangle}$. It is known that higgs boson production at LHC by the weak boson fusion mechanism is itself suppressed relative to the gluon fusion mechanism over most of the range of M_h ($M_h < 1$ TeV). Hence the radion production at LHC by weak boson fusion is also not expected to be the dominant or efficient mechanism. Also the radion couplings to light valence quarks are extremely small. Therefore in this article we shall focus on radion production by gluon fusion. The radion production cross-section at a hadron collider *via* gluon fusion mechanism is given by,

$$\sigma(p\,p(\bar{p}) \to \tilde{\phi} + X) = \Gamma(\tilde{\phi} \to gg)\,\frac{\pi^2}{8m_{\tilde{\phi}}^3}\,\tau \int_\tau^1 \frac{dx}{x}\,g(x)\,g(\frac{\tau}{x}) \tag{7}$$

Here τ is a dimensionless variable given by $\frac{m_{\tilde{\phi}}^2}{S}$, where S is the proton - proton (anti-proton) center of mass energy. Note that $L_{\phi gg}$ generates momentum dependent $\tilde{\phi}gg$, $\tilde{\phi}ggg$ and $\tilde{\phi}ggg$ couplings. The strength of these couplings are proportional to $\beta(g_s)$ which includes the contribution of gluons as well as the dynamical quarks. The Lagrangian also indicates that radions could be produced either singly or in association with gluons at a hadron collider by gluon fusion. In fact the gluon fusion mechanism turns out to be the dominant production process for radions at hadron colliders over most of the interesting range. $qg \to \tilde{\phi}$ and $\bar{q}g \to \tilde{\phi}$ does make a small contribution to radion production in $O(\alpha_s)^3$. The radion coupling to gluons is very similar in structure to the effective Lagrangian that gives the higgs coupling to gluons [5] in the heavy quark limit. As in the case of the radion the gluon fusion also turns out to be the primary production mechanism for higgs boson at hadron collider. The dominant contribution to $gg \to h$ arises from closed loops of heavy quarks that occur in the theory. In this work we shall assume that the number of heavy

quarks (N_h) is equal to one namely the top. It has been shown [6] that the heavy quark limit $\frac{M_h}{M_q} \to 0$ is an excellent approximation to the exact two loop corrected rate for $gg \to h$. As $m_h \to 2\ m_t$ the exact result rises above the heavy quark result and exhibits a small bump corresponding to the $t\bar{t}$ threshold. The width of the bump *i.e* the departure region increases with increasing m_t. The disagreement between the two results in the $m_h \geq 2m_t$ region however is always less than a factor of two at LHC. The heavy quark limit for $gg \to h$ can be obtained from the gauge invariant effective Lagrangian [7]

$$\mathcal{L} = -\frac{1}{4}\left[1 - \frac{2\ \beta_h}{g_s(1+\delta)}\ \frac{h}{v}\right] G^a_{\mu\nu} G^{a\mu\nu} - \frac{m_t}{v}\ h\bar{t}t. \tag{8}$$

$\delta = 1 + 2\frac{\alpha_s}{\pi}$ is the anomalous dimension of the mass operator arising from QCD interactions. β_h is the heavy quark contribution to the QCD beta function. Since the hgg coupling in the $M_q \to \infty$ limit arises from heavy quark loops it is only the heavy quarks that contribute to the β_h in eqn(3). To order (α_s^3) the heavy quark contribution [6] to $\beta(g_s)$ is given by $\beta_h = N_h \frac{\alpha_s}{12\pi}[1 + \frac{19\alpha_s}{4}]$. On the other hand the $\beta(g_s)$ that appears in the gluon coupling to the dilaton like radion mode arises from the trace anomaly. The trace anomaly has its origin in the heavy regulator fields as their masses are taken to infinity. So it includes the gluonic contribution as well as that of dynamical quarks. This difference in the two beta function contributions makes the $\tilde{\phi}gg$ coupling greater than the hgg coupling even for $\frac{v}{\langle\phi\rangle} = \frac{1}{4}$. However with increasing $\langle\phi\rangle$ the hgg coupling ultimately wins over the $\tilde{\phi}gg$ coupling. This feature is clear from fig. 2 where it is shown that with increasing $\langle\phi\rangle$, $\sigma(pp \to \tilde{\phi})$ ultimately becomes smaller than $\sigma(pp \to h)$.

Let us now make some rough numerical estimate about the ratio $\frac{\sigma(pp\to\phi)}{\sigma(pp\to h)}$ in the lowest order ($\mathrm{O}(\alpha_s)$). Our estimates will depend only on the relative strength of ϕgg and hgg couplings. For $\sqrt{\hat{s}} < 2m_t$, $\frac{\beta(g_s)}{2g_s} = -3.84\frac{\alpha_s}{4\pi}$ whereas $\beta_h = \frac{1}{3}\frac{\alpha_s}{4\pi}$ to lowest order. Also in this region the heavy quark limit provides a good approximation to the exact result for $\sigma(pp \to h)$. We find that $\frac{g_{gg\phi}}{g_{ggh}} \approx -2.88$ for $\langle\phi\rangle = 1$ TeV. Above the $2m_t$ threshold we have $\frac{\beta(g_s)}{2g_s} \approx -3.50\frac{\alpha_s}{4\pi}$. Although in this region the heavy quark limit does not work that well for the higgs cross section we can still get an order of magnitude estimate (lower by at most a factor of two) using it. The ratio of couplings now ($\sqrt{\hat{s}} > 2m_t$) becomes $\frac{g_{gg\phi}}{g_{ggh}} \approx -2.63$.

Using the fact that the effective Lagrangian for higgs and radion production by gluon fusion are similar except for couplings we find that if $\langle\phi\rangle$=1 TeV then the cross section for $pp \to \tilde{\phi}$ will exceed that of $pp \to h$ by a factor of 8.3 for $\sqrt{\hat{s}} < 2m_t$ and by a factor of 6.9 for $\sqrt{\hat{s}} > 2m_t$. However for $\langle\phi\rangle$=5 TeV the radion production cross section will be suppressed relative to the higgs cross section roughly by a factor of three. These features have been exhibited in fig. 2 where we have plotted the lowest order higgs production cross section (both

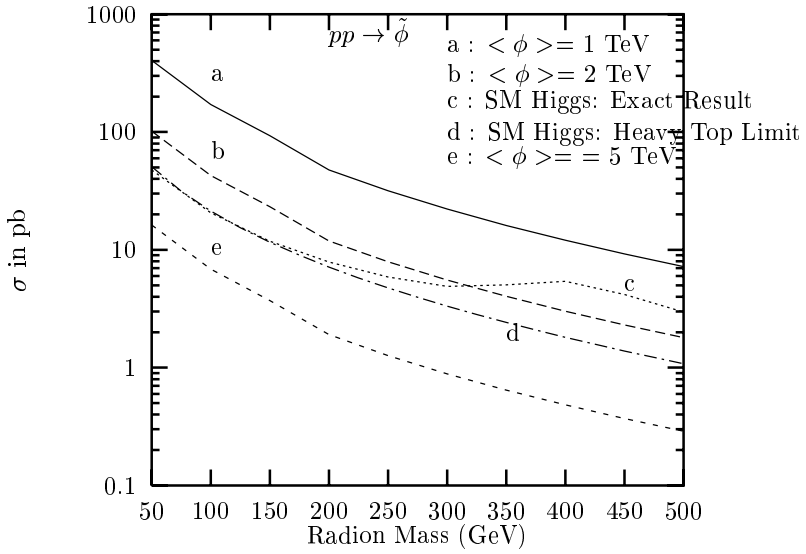

Figure 2: *Radion production cross-section (a,b,e) at the LHC, for different values of $\langle\phi\rangle$. We also present the SM higgs production cross-section (c) the exact result and (d) in the heavy quark limit.*

exact and the heavy quark limit) and the radion cross section (for three different values of $\langle\phi\rangle$) against the mass of the particle ($\tilde{\phi}$ or h) at LHC.

The estimates given above are based on lowest order calculations. It is known that higher order QCD corrections increases the lowest order rate by a factor (K factor) that lies between 2 and 3 at LHC [6, 8]. The QCD radiative corrections done in the heavy quark limit forms an excellent approximation to the exact calculations. To calculate the K factor one therefore always uses the heavy quark limit. But in the heavy quark limit the effective Lagrangian for higgs production is similar in structure to the Lagrangian for radion production. Hence the K factor for higgs production in the heavy quark limit will be the same for the radion also. So higher order QCD corrections will not affect the relative rate between the radion and the higgs to a very high degree of accuracy.

3 Detection and Possible SM Backgrounds

Let us now concentrate on the detection of radion at a hadron collider like Tevatron. The dominant decay mode of a 50-150 GeV radion as can be seen from fig. 1, is to $b\bar{b}$ or to gg. But the striking feature is that the $\gamma\gamma$ branching ratio of the radion is larger than the higgs case by a factor 5-8, over a considerable mass range. The higgs production rate by gluon fusion and and its decay into the $\gamma\gamma$ mode are both suppressed relative to that of the radion. This is the reason why two photon final state is not a good bet for the higgs at the Tevatron.

At the Tevatron radion production cross-section varies from 140 pb to 1 pb as we vary radion mass from 20 (current lower bound on radion mass comes from LEP -II [9]) to 160 GeV. We have included a NLO QCD correction factor of 2 in our calculation. This cross-section with the presently collected luminosity will give rise to some 10 ^{4} radions. If the radion decays into the $\gamma\gamma$ mode the final state will consist of 2 hard photons. The main background of this 2-photon final state comes from the pair annihilation of the valence quarks and anti-quarks. The other dominant source of $\gamma\gamma$ background is gluon gluon annihilation to two photons. Though this is suppressed to the former by a factor of α_s^2, dominance of gluon flux over the quarks flux, can make this comparable with the former. We do not calculate this second contribution explicitly. We multiply the $q\bar{q} \to \gamma\gamma$ contribution by a factor of 2 to take this into account. At the Tevatron this is a conservative approximation. We have used a parton level monte-carlo event generator to estimate the numbers for both the signal and the background and the CTEQ-4M [10] parametrisation for the parton densities in our entire analysis.

The following cuts have been applied to differentiate between signal and background.
$p_T^\gamma > 10$ GeV
We demand the photons are in the central part of the detector.
$|\eta_\gamma| < 3.$.
We also require that the angular separation between the photons be substantial, *i.e.* $\Delta R_{jj} \equiv \sqrt{(\Delta\eta_{\gamma\gamma})^2 + (\Delta\phi_{\gamma\gamma})^2} > 0.5$

Even after applying these cuts, the SM background cannot be removed completely. So the strategy is to compare the invariant mass (of the photon pair) distribution of the signal and background. For the signal (of a definite $m_{\tilde{\phi}}$), invariant mass distribution shows a sharp peak over the continuum background. The sharpness of the peak depends mainly on the detector resolution and the partial width of $\tilde{\phi} \to \gamma\gamma$. In fig. 3 we plot the invariant mass ($M_{\gamma\gamma}$) distribution for the signal (dots) and backgrounds (broken histogram) assuming an uniform bin size of 5 GeV. Here one can see that, for low $M_{\gamma\gamma}$, number of background events is higher than the signal. But as $M_{\gamma\gamma}$ increases, the number of background events in the mass bins falls off more rapidly than the signal- which more or less remains the same over the entire mass range we are interested here. Once the radion mass is near to $2m_w$, signal events falls off sharply, due to the

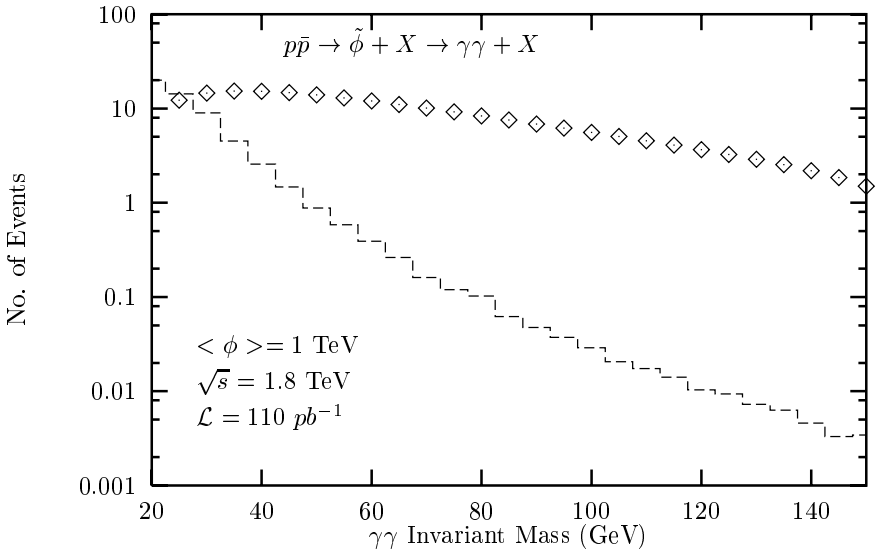

Figure 3: *Invariant mass distribution for signal and background at the Tevatron for $\langle\phi\rangle$ = 1 TeV.*

sharp fall of $\gamma\gamma$ branching ratio.

We find that the $\gamma\gamma$ mode is good enough to exclude radion mass nearly upto 120 GeV even with the presently collected luminosity of 110 pb^{-1}. Here we have taken the radion *vev* to be 1 TeV. On the other hand at the Tevatron with the presently collected luminosity one cannot say anything about the SM higgs.

Now let us go over to the case of Upgraded Tevatron with center of mass energy of 2 TeV and luminosity of 1 fb^{-1}. As center of mass energy is almost equal to the present, the signal and background are just 10 times larger than the previous case. This is evident from the fig. 4. In this figure we also plot the significance ($\equiv \frac{No.of Signal}{\sqrt{No.of Background}}$) of our signal upto $M_{\gamma\gamma}$ equal to 100 GeV. One can check, over this entire mass range, significance is greater than 5. Generally a significance greater than 5 points to the discovery. One can also easily check that once $M_{\gamma\gamma}$ is greater than 100 GeV, no. of background events

in the corresponding bins become less than 1 events. So in this region we can demand 5 signal events as a benchmark for discovery. Thus at the upgraded Tevatron one can discover radion mass upto 160 GeV and exclude upto 165 GeV. Once $M_{\gamma\gamma}$ is greater than 165 GeV, our signal falls off very sharply and we cannot say anything more about it.

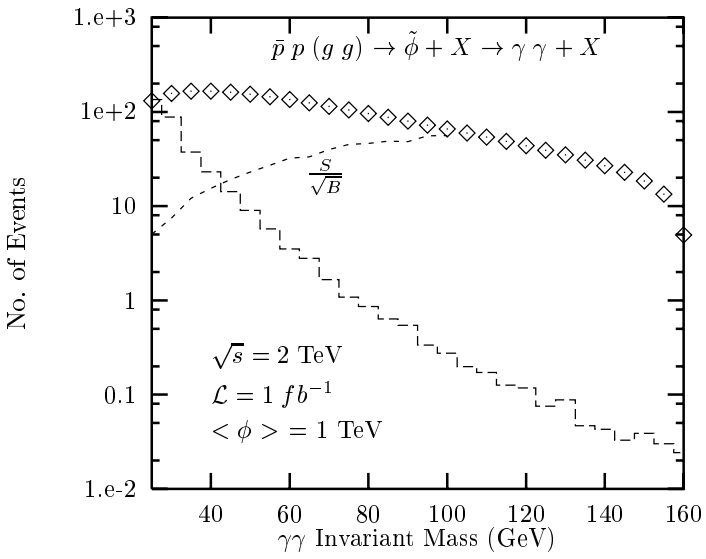

Figure 4: *Invariant mass distribution for signal and background at the Tevatron Upgrade for $\langle\phi\rangle$ = 1 TeV.*

If we change $\langle\phi\rangle$ the branching ratio of the radion to different channels remains same. So if we take $\langle\phi\rangle = 2$ TeV, the cross-section and number of $\gamma\gamma$ events become $\frac{1}{4}$ of the present case ($\langle\phi\rangle = 1$ TeV). And at the Tevatron with the presently collected luminosity, we cannot say anything about it. At the Tevatron Upgrade, we also cannot talk about the discovery, for $m_{\tilde{\phi}}$ <45 GeV. At higher masses, one can discover upto 150 GeV m_ϕ if $\langle\phi\rangle = 2$ TeV instead of 1 TeV.

Finally we want to examine the search prospects of this scalar particle at the LHC. Though the two photon branching ratio drops very sharply near $m_{\tilde{\phi}} \sim$ 140 GeV, in contrast to the SM case it remains constant with $m_{\tilde{\phi}}$ after 140

GeV. Also the radion production rate is almost 8 times higher than that of higgs production rate. So unlike the SM higgs boson, for $m_{\tilde{\phi}} > 140$ GeV, $\gamma\gamma$ mode is a viable avenue to discover or exclude the radion for masses well upto 1 TeV.

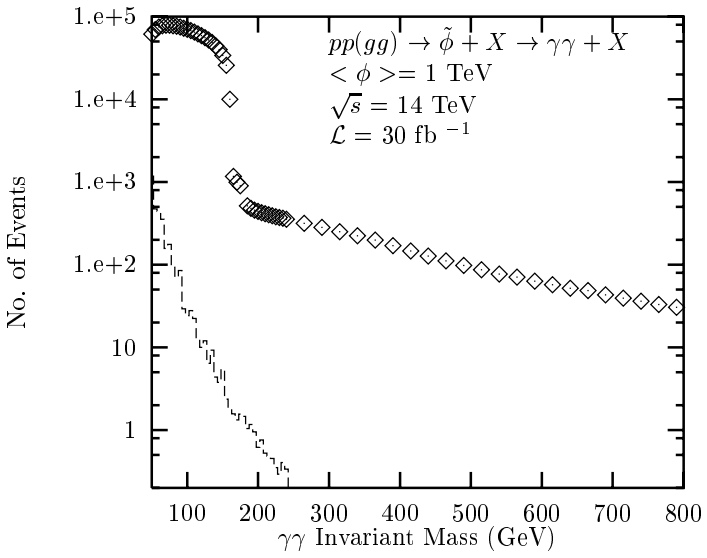

Figure 5: *Invariant mass distribution for signal and background at the LHC for* $\langle\phi\rangle = 1$ *TeV.*

Conservatively, we take the luminosity to be equal to 30 fb^{-1}. The source of SM backgrounds remain the same here. But unlike the Tevatron, the 2-photon background coming from pair annihilation of quark and anti-quark becomes less severe. This is because the anti-quark coming from one proton has to be excited from the sea. But gluon density in the proton is much larger than the quark density at LHC. So to take into account the gluon gluon contribution to 2-photon background we multiply the quark-anti-quark contribution by a factor of 6 [1]. The cuts we used here are rather similar to the Tevatron case. Only we

[1] Generally at the LHC energies the gluon-gluon contribution to two photon background is 5 times larger than the quark anti-quark contribution. For $m_{\gamma\gamma} = 110$ (130) GeV this factor

change the cuts on the transverse momenta of the photons to be greater than 20 GeV. We present in fig. 5 the number of signal events and the corresponding number for the background against the $\gamma\gamma$ invariant mass. To plot the invariant mass distribution for the background we choose a bin size of 5 GeV. Form the figure one can easily see that the background is an order of magnitude smaller than the signal over the entire mass range. And once $M_{\gamma\gamma}$ is greater than 250 GeV, there are less than one event in the respective mass bins. That's why we do not show it in the figure. So LHC can easily discover radions with masses upto 1 TeV for $\langle\phi\rangle$=1 Tev. If we increase $\langle\phi\rangle$ to 4 TeV one can easily check from fig. 5 that our discovery limit comes down to 650 GeV.

4 Conclusions

In this paper we examined the radion production and its subsequent decay into SM particles at hadron colliders. The radion production cross-section is larger than the higgs production cross-section by a factor of 6-8. The partial width of the radion to two gluons and two photons is also enhanced due to the enhanced $\tilde{\phi}\ g\ g$ or $\tilde{\phi}\ \gamma\ \gamma$ coupling. The other partial widths are suppressed with respect to higgs widths by a factor that depends on $\langle\phi\rangle$. We also discussed the viability of the 2-photon signal for the radion at the Tevatron. One can exclude radion mass upto 120 GeV even with the presently collected luminosity. Upgraded Tevatron with higher center of mass energy and higher luminosity certainly can discover radion upto 160 GeV mass, if not it can exclude it upto 165 GeV. Similarly at the LHC one can definitely discover radions with masses up to 1 TeV. These estimates are done assuming $\langle\phi\rangle$ =1 TeV. With increasing $\langle\phi\rangle$ both the exclusion limit and the discovery limit using the $\gamma\gamma$ mode will come down.

Note added: While this work was being completed there appeared one paper [12] which discusses some of the issues presented here.

References

[1] L. Randall and R Sundrum, *Phys. Rev. Lett.* **83**, 3370 (1999).

[2] W. D. Goldberger and M. B. Wise, Phys. Rev. Lett. 83, 4922 (1999); *Phys. Rev.* **D60**, 107505 (1999).

[3] C. Csaki, M. Graesser, L. Randall and J. Terning, hep-ph/9911406; W. D. Goldberger and M. B. Wise, hep-ph/9911457.

has been estimated to be 3.55 (3.56) for the LHC [11].

[4] J. C. Collins, A. Duncan and S. D. Joglekar, *Phys. Rev.* **D16**, 438 (1977).

[5] M. Acciari *et al.* The L3 *Collab.*; *Phys. Lett.* **B 461**, 367 (1999).

[6] S. Dawson, *Nucl. Phys.* **B359**, 283 (1991).

[7] A. Vainshtein, M. Voloshin, V. Zakharov and M. Shifman, *Sov. J. Nucl. Phys.* **30**, 711 (1979); A. Vainshtein, V. Zakharov and M. Shifmsn,*Sov. Phys. Usp.* **23**, 429 (1980).

[8] A. Djouadi, M. Spira and P. Zerwas, *Phys. Lett.* **B 264**, 440 (1991).

[9] U. Mahanta and S. Rakshit, hep-ph/0002049.

[10] H. L. Lai et al., Phys. Rev. **D55**, 1280 (1997).

[11] CMS Collaboration, G.L. Bayatian *et al.*, Technical Proposal CERN/LHCC 94-38 (December 1994).

[12] G. F. Giudice, R. Rattazzi, J. D. Wells; hep-ph/0002178.